INVESTIGATION OF BACK-PROPAGATION NETWORK STRUCTURES IN PREDICTING WEAR VALUE OF CBN-COATED TOOLS DURING HIGH-SPEED DRY TURNING OF SKD11 STEEL

Hoang Thi Dieu[1,*], Tang Quoc Nam[2], Phung Van Binh[2], Dao Van Duong[3], Nguyen Van Trung[4]

DOI: http://doi.org/10.57001/huih5804.2024.162

ABSTRACT

This paper presents the results of surveying the effect of backpropagation network structures on the predictive quality of CBN-coated cutting tools in high-speed dry turning of SKD11 steel on CNC machines. Based on the analysis of the back-propagation network (BPN) characteristics and determining that the number of hidden layers of this network structure is fixed, eighteen network structures corresponding to the six ratios of the number of neurons between the hidden layers are investigated and evaluated. The network training dataset is collected from 280 high-speed turning experiments with four input variables and one output variable. The network quality evaluation criteria include R^2, MSE, RMSE and MAPE indexes. The survey results show that, in this particular case study, the ratio of the number of neurons between hidden layer 1 and hidden layer 2 reaches 1:2, giving the best prediction quality. The 4-10-20-1 network configuration is the model for the best quality. The research results can serve as a basis for selecting the appropriate neural network (NN) configuration for models with large amounts of data and many input variables. However, this study only examines the network model with 2 hidden layers.

Keywords: *Backpropagation; Dry turning; Neural networks; Tool wear.*

[1]Nam Dinh University of Technology Education, Vietnam
[2]Le Quy Don Technical University, Vietnam
[3]Dong Nai University, Vietnam
[4]Lac Hong University, Vietnam
[*]Email: hoangdieunute@gmail.com
Received: 05/8/2023
Revised: 07/10/2023
Accepted: 25/5/2024

1. INTRODUCTION

Wear and failure of cutting tools are serious problems in cutting in general and high-speed machining of high hardness materials in particular. Tool wear accounts for about 20% of total machine downtime, resulting in dramatic increases in production costs [1]. In recent decades, hard turning technology has been studied to replace grinding technology in finish machining hardening steel products [2-4]. During hard turning, thanks to the single-blade tool it is possible to precisely adjust the cutting angle and thus easily machine complex surfaces of the product. Moreover, hard turning can also perform dry machining [5, 6] without cool fluids, so it does not affect the environment and workers' health [7]. The problem of tool wear and damage requires special attention in hard turning, especially when machining at high speed. It is now more important than ever to build models to predict tool wear.

The rapid development of computer science has made artificial intelligence (AI) networks a popular choice for building predictive models. The efficiency of the application of artificial neural networks (ANN) compared with other prediction methods is also compared as shown in [8, 9]. Different types of NN such as forward propagation networks [10, 11], convolutional networks [12], back-propagation networks are popularly and widely used by scientists based on the superiority of and their effectiveness [13, 14]. There are a number of methods to help ANN improve prediction accuracy such as using BPN with Gradient Descent (GD) technique [13-17]. The BPN model is presented in [13] to build a model to predict tool wear in turning hardening H13 steel. The predictive model of cutting heat, cutting force and tool wear is built based on BPN model in [14] when dry turning of Nimonic C263 alloy. Two-dimensional objects are recognized in the study [15] with BPN model and fuzzy clustering technique. The features of the objects are efficiently predicted by the BPN model after they are classified. The traditional back-propagation network model and the improved BPN model reviewed and compared in [16] showed their effectiveness in predicting risk factors associated with hypertension in patients. A geometrical interpretation of the morphological BPN is described in [17] with a proposed set of rules for continuously updating the NN parameters.

This paper focuses on determining the influence of BPN structures on the predictive quality of tool wear values in dry high-speed turning for SKD11 steel. The network structures are fixed in terms of the number of hidden layers of neurons, and the number of neurons in each of these hidden layers is changed at specific rates. The model evaluation criteria are determined to find out the percentage of neurons in the

classes that give the best quality prediction results. Based on that, a specific BPN structure is determined. The results of evaluation and comparison can be used as a basis for building similar network structures in the future.

2. RESEARCH CONTENTS

2.1. Experimental setup

Experiments were carried out on a lathe HAAS-ST10. Select SKD11 steel workpieces that has been heat treated to reach hardness 54÷56HRC, workpiec length is 300mm, workpiece diameter is 30mm (Fig. 1). The chemical composition of the workpieces is described in Table 1.

Table 1. Material composition SKD11

Ingredient	C	Si	Mn	Cr	Ni	Mo	Va
%	1.45 - 1.65	≤ 0.4	≤ 0.35	11.0 - 12.5	0.25 - 0.4	0.4 - 0.6	0.15 - 0.3

For cutting tools, choose the CBN insert piece with symbol TNP-VNGA168408G2 (MB8025) of Mitsubishi with specifications including IC = 9.525mm (Insert IC Size); LE = 16.606mm (Insert Cutting Edge Length); S = 4.76mm (Insert Thickness); RE = 0.8mm (Corner Radius); D1 = 3.81mm (Insert Hole Size). The tool wear value was determined after each machining interval with the help of an electron microscope UM012C with the help of MicroCapture software on the background of digital images taken and record once. The test is stopped when the tool wear height reaches $VB_{max} \geq 0.6$(mm). At that time, the new turning tool insert will be replaced. Each experiment used one insert piece. The experimental system is depicted as shown in Fig. 2. The experiments were carried out with the set of cutting parameters recommended by the cutting tool supplier and through some preliminary tests. The technical parameters are described in Table 2.

Table 2. Cutting parameters

Parameters	Level 1	Level 2	Level 3
V_C(mm/min)	80	125	170
f(mm/rev)	0.07	0.11	0.15
a_P(mm)	0.1	0.25	0.175

Fig. 1. Turning workpiece SKD11

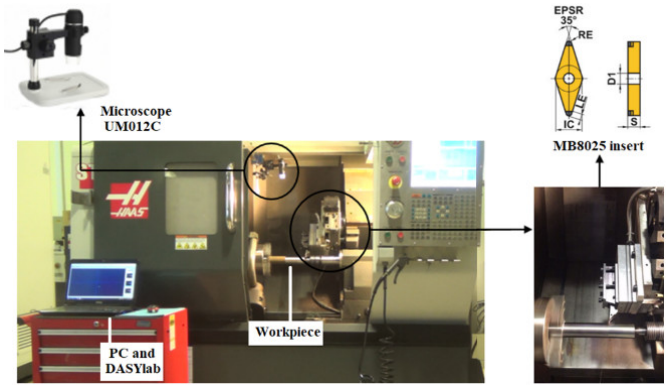

Fig. 2. Machining and measuring systems

2.2. Back-propagation network model

The BPN model uses the GD algorithm to continuously adjust the coefficients b_i and w_i through the loss function derivative from the last layer to the first layer [13, 14]. The final layer is precomputed because its value is close to the predicted output value and loss function value. The calculation of the derivative of the previous classes is done based on the "Chain rule". The derivative value is calculated for each specific consecutive point of the function, the algorithm will stop when the loss function value reaches the minimum. The implementation steps of the algorithm can be described as shown in Fig. 3.

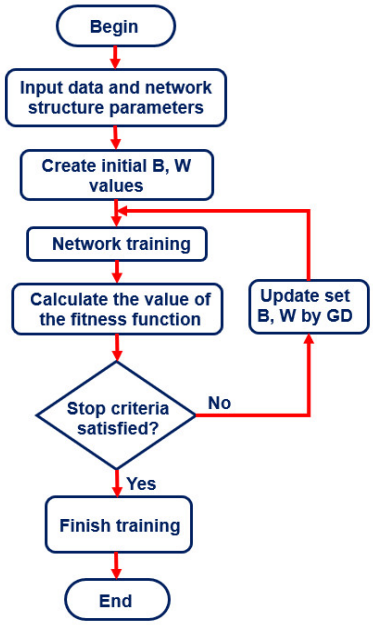

Fig. 3. Diagram of BPN algorithm using GD

The advantage of the BPN model using the GD algorithm is that it avoids the phenomenon of "high bias" (this is the case where the optimal set of parameters b_i and w_i are found too fast and satisfies the global optimal value, the entire iteration of the optimization algorithm only receives a single set of b_i and w_i values. This leads to the final ANN being unreliable enough to conclude). The limitation of this method is evident when the loss function is complicated or the structure of the ANN is complex.

The indexes R^2 [18], MSE [19], RMSE [20, 21] and MAPE [22] were used to evaluate the training quality of ANN. The R^2 index is determined as follows

$$R^2 = 1 - \left(\frac{\sum_{i=1}^{N} (y_{pi} - y_{ri})^2}{\sum_{i=1}^{N} y_{pi}^2} \right)$$

In which, y_{pi} and y_{ri} are the predicted and actual tool wear values in experiment i., respectively. The total number of experiments is N.

The MSE index is calculated as follows

$$MSE = \frac{1}{N} \sum_{i=1}^{N} (y_{pi} - y_{ri})^2$$

Similar to the MSE, the RMSE index is described as follows

$$RMSE = \sqrt{\frac{1}{N} \sum_{i=1}^{N} (y_{pi} - y_{ri})^2}$$

The MAPE index is used to measure the performance or degree of error between the predicted dataset and the actual dataset. This indicator is expressed as follows

$$MAPE = \frac{1}{N} \sum_{i=1}^{N} \left(\left| \frac{y_{pi} - y_{ri}}{y_{ri}} \right| \right) \times 100\%$$

2.3. Analysis results and discussion

The BPN network models are built with input layer, hidden layers and output layer described similar to Fig. 4.

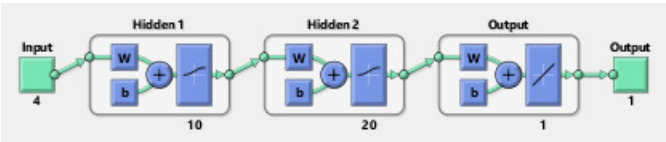

Fig. 4. Structure illustration of 4-10-20-1 network

The input layer has 4 variables including cutting speed (Vc - m/min), feed rate (f - mm/rev), depth of cut (a_p - mm) and machining time (Time - seconds). The output layer has 1 variable which is the tool wear value (VB - mm). The specific parameters are presented in Table 3.

Table 3. BPN model structure parameters

No	Parameters	Values
1	Number of input layer variables	7
2	Number of output layer variables	1
3	Number of neurons in hidden layer 1	5
4	Number of neurons in hidden layer 2	10
5	Data Split Ratio: Training/ Validation/ Testing	80%/10%/10%
6	Number of experiments	289
7	Transfer function	Logsig
8	Training function	traingdx
9	Maximum number of epochs to train	10000
10	Fitness function	MSE
11	Learning rate	0.01
12	Ratio to increase learning rate	1.05
13	Ratio to decrease learning rate	0.7
14	Momentum constant	0.9

Assuming the number of hidden layers of the BPN is fixed, the ratio of neurons between the hidden layers changes as follows: (1:1), (1:2), (1:3), (1:4), (1:5), (1:6) correspond to the structures described in Table 4.

Table 4. Number of neurons in hidden layers with respective ratios

Cases	Number of hidden layer neurons 1	The number of neurons in the hidden layer 2 corresponds to the ratio					
		1:1	1:2	1:3	1:4	1:5	1:6
Case 1	5	5	10	15	20	25	30
Case 2	10	10	20	30	40	50	60
Case 3	15	15	30	45	60	75	90

The experimental dataset with actual measurement results is described in the Appendix. The results of the evaluation of the BPN model quality of the steps with Case 1 for all experimental data are shown in Table 5.

Table 5. Network quality assessment results with 5 neurons in hidden layer 1 (Case 1)

Criteria	Ratio of hidden layer neurons 1 and 2					
	1:1	**1:2**	1:3	1:4	1:5	1:6
R^2	0.982	**0.983**	0.982	0.98	0.978	0.978
MSE ($x10^{-4}$)	5.77	**5.52**	5.85	6.31	7.03	6.92
RMSE	0.024	**0.023**	0.024	0.025	0.026	0.026
MAPE (%)	10.16	**8.7**	11.35	10.78	11.46	11.22

The results of the evaluation of BPN model quality in stages with Case 2 for all experimental data are presented in Table 6.

Table 6. BPN quality assessment results with 10 neurons in hidden layer 1 (Case 2)

Criteria	Ratio of hidden layer neurons 1 and 2					
	1:1	**1:2**	1:3	1:4	1:5	1:6
R^2	0.983	**0.983**	0.982	0.977	0.978	0.976
MSE ($x10^{-4}$)	5.49	**5.6**	5.56	7.06	7.08	7.65
RMSE	0.023	**0.023**	0.023	0.027	0.027	0.028
MAPE (%)	12.75	**8.59**	9.45	10.05	10.53	9.95

The results of the evaluation of BPN model quality in stages with Case 3 for all experimental data are presented in Table 7.

Table 7. BPN quality assessment results with 15 neurons in hidden layer 1 (Case 3)

Criteria	Ratio of hidden layer neurons 1 and 2					
	1:1	**1:2**	1:3	1:4	1:5	1:6
R^2	0.9827	**0.983**	0.98	0.978	0.98	0.979
MSE ($x10^{-4}$)	5.59	**5.35**	6.46	7.05	6.36	6.76
RMSE	0.023	**0.023**	0.025	0.026	0.025	0.026
MAPE (%)	10.71	**8.89**	10.94	9.94	9.9	9.72

Some observations can be considered as follows

- The ANN with a ratio of neurons between hidden layers of 1:2 gives the best prediction quality.

- The MSE value in Case 3 is the smallest ($5.35x10^{-4}$). Considering the MAPE value, Case 2 gives the lowest value (8.7). But the MSE value in Case 2 ($5.6x10^{-4}$) is higher than in Case 1 ($5.52 x10^{-4}$). It is easy to see that the MSE difference between the cases is very small. Therefore, the underlying RMSE value is the same.

- If considering each indicator, each case has a superior indicator.

- Case 1 shows that the number of bi coefficients and weights wi is the smallest because the number of neurons in each hidden layer is the smallest. Therefore, the number of variables of the BPN network is the least in the cases considered.

Accordingly, network models with the ratio of neurons between hidden layer 1 and hidden layer 2 reaching 1:2 give the best prediction results. These include: 4-5-10-1 (in Case 1), 4-10-20-1 (in Case 2) and 4-15-30-1 (in Case 3). Table 8 compares the values of the criteria for each case in different training stages.

Table 8. Evaluation criteria at different stages for 3 best cases

Criteria	Traning process			Test process			All data		
	Case 1	Case 2	Case 3	Case 1	Case 2	Case 3	Case 1	Case 2	Case 3
R2	0.987	**0.987**	0.985	0.927	**0.981**	0.973	0.983	**0.983**	0.983
MSE ($x10^{-4}$)	4.06	**4.01**	5.14	7.52	**5.66**	6.41	5.52	**5.6**	5.35
RMSE	0.02	**0.02**	0.023	0.044	**0.024**	0.025	0.023	**0.023**	0.023
MAPE (%)	8.083	**7.6**	8.24	13.84	**10.44**	9.72	8.7	**8.59**	8.89

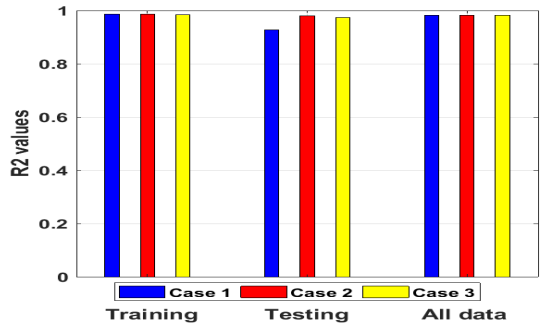

Fig. 5. R^2 index values in respective periods

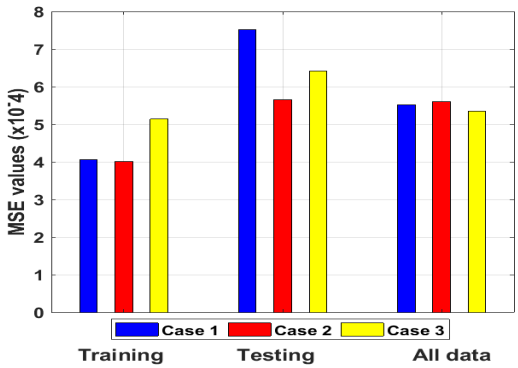

Fig. 6. Values of MSE in respective periods

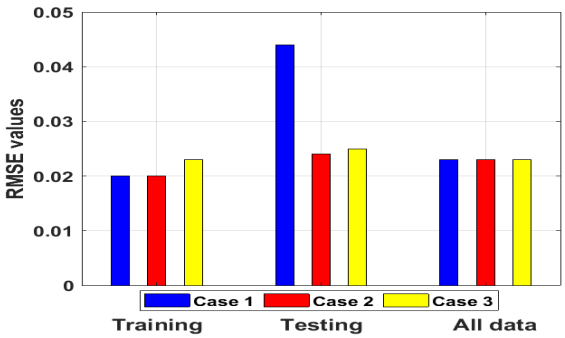

Fig. 7. RMSE values in respective periods

The R^2 value of the model 4-10-20-1 in the verification period reached the largest (0.981). Fig. 5 visually illustrates the value of this indicator in each specific case. According to Tab. 8, MSE values ($4.01x10^{-4}$) and MAPE (7.6%) of Case 2 reached the lowest in the training period and are depicted in Fig. 6 and Fig. 8, respectively. RMSE error reached the highest during the training period. verification phase (0.044) with the 4-5-10-1 model (Fig. 7).

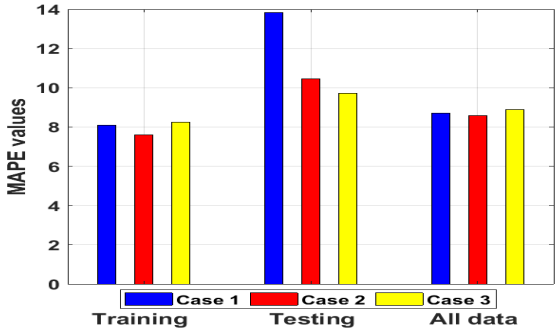

Fig. 8. MAPE value in respective periods

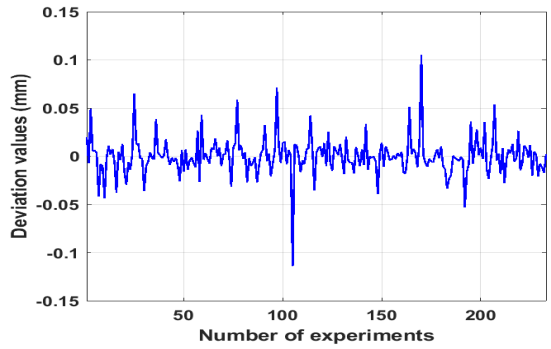

Fig. 9. Difference between actual and predicted tool wear in training process

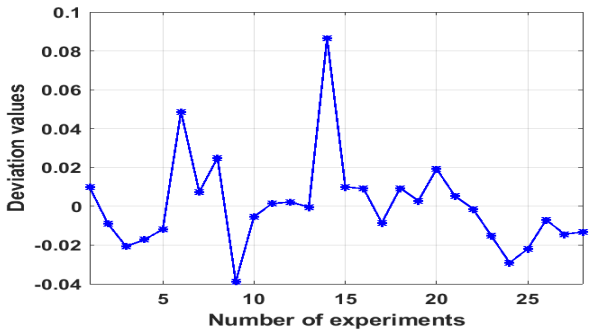

Fig. 10. Difference between actual and predicted tool wear in testing process

Fig. 9 and Fig. 10 depict the difference between the actual measured value and the predicted value in the training and verification phases, respectively. Accordingly, the largest deviation value in these two phases is 0.12mm and 0.09mm, respectively.

In summary, based on the calculation results in Table 8, the BPN model configuration with the structure 4-10-20-1 gives the best quality prediction results.

3. CONCLUSIONS

In this paper, all 18 back-propagation network configurations with 2 hidden layers, 4 input variables and 1 output are investigated to determine the network structure for the best prediction quality. The wear value of CBN coated cutting tools in high-speed dry turning of hardened steel SKD11 is the predicted target. Based on the calculation results of R^2, MSE, RMSE and MAPE indexes, the network structure with the number of neurons between hidden layer 1 and hidden layer 2 reached the ratio 1:2 for the best prediction results. Based on that, the 4-10-20-1 network structure is considered to be the most suitable in this particular case study. Basically, most of the quality evaluation criteria are quite close to each other, the main difference lies in the MAPE index with the balanced evaluation characteristics of the weights among the variables in the ANN. This research result is suitable for problems with corresponding data sets of input, output and number of hidden layers.

REFERENCES

[1]. Kurada S., Bradley C., "A review of machine vision sensors for tool condition monitoring," *Computers in industry*, 34(1), 55-72, 1997.

[2]. Orra K., Choudhury S. K., "Development of flank wear model of cutting tool by using adaptive feedback linear control system on machining AISI D2 steel and AISI 4340 steel," *Mechanical systems and signal processing*, 81, 475-492, 2016.

[3]. Özel T., Karpat Y., Figueira L., Davim J. P., "Modelling of surface finish and tool flank wear in turning of AISI D2 steel with ceramic wiper inserts," *Journal of materials processing technology*, 189(1-3), 192-198, 2007.

[4]. Niaki F. A., Michel M., Mears L., "State of health monitoring in machining: Extended Kalman filter for tool wear assessment in turning of IN718 hard-to-machine alloy," *Journal of Manufacturing Processes*, 24, 361-369, 2016.

[5]. Sanchez Y., Trujillo F. J., Sevilla L., Marcos M., "Indirect monitoring method of tool wear using the analysis of cutting force during dry machining of Ti alloys," *Procedia Manufacturing*, 13, 623-630, 2017.

[6]. Caggiano A., Napolitano F., Teti R., "Dry turning of Ti6Al4V: tool wear curve reconstruction based on cognitive sensor monitoring," *Procedia CIRP*, 62, 209-214, 2017.

[7]. Poulachon G., Bandyopadhyay B. P., Jawahir I. S., Pheulpin S., Seguin E., "Wear behavior of CBN tools while turning various hardened steels," *Wear*, 256(3-4), 302-310, 2004.

[8]. Özel T., Karpat Y., "Predictive modeling of surface roughness and tool wear in hard turning using regression and neural networks," *International journal of machine tools and manufacture*, *45*(4-5), 467-479, 2005.

[9]. Tangjitsitcharoen S., "Comparison of Neural Networks and Regression Analysis to Predict In-process Straightness in CNC Turning," *Procedia Manufacturing*, *51*, 222-227, 2020.

[10]. Liu Q., Altintas Y., "On-line monitoring of flank wear in turning with multilayered feed-forward neural network," *International Journal of Machine Tools and Manufacture*, *39*(12), 1945-1959, 1999.

[11]. Pant P., Chatterjee D., "Prediction of clad characteristics using ANN and combined PSO-ANN algorithms in laser metal deposition process," *Surfaces and Interfaces*, 21, 100699, 2020.

[12]. García-Pérez A., Ziegenbein A., Schmidt E., Shamsafar F., Fernández-Valdivielso A., Llorente-Rodríguez R., Weigold M., "CNN-based in situ tool wear detection: A study on model training and data augmentation in turning inserts," *Journal of Manufacturing Systems*, 68, 85-98, 2023.

[13]. Özel T., Nadgir, A., "Prediction of flank wear by using back propagation neural network modeling when cutting hardened H-13 steel with chamfered and honed CBN tools," *International Journal of Machine Tools and Manufacture*, 42(2), 287-297, 2002.

[14]. Ayyaswamy J. P. K., Kulandaivel A., Ezilarasan C., Arunagiri A., Charles M., Kumar S. R., "Predictive model development in dry turning of Nimonic C263 by artificial neural networks," *Materials Today: Proceedings*, *59*, 1284-1290, 2022.

[15]. Wu W. Y., "A Back-Propagation Neural Network for Recognizing Objects," *European Journal of Engineering and Technology Research*, 7(5), 102-109, 2022.

[16]. Yan Y., Chen R., Yang Z., Ma Y., Huang J., Luo L., Yu H., "Application of back propagation neural network model optimized by particle swarm algorithm in predicting the risk of hypertension," *The Journal of Clinical Hypertension*, 24(12), 1606-1617, 2022.

[17]. Groenendijk R., Dorst L., Gevers T., "Geometric back-propagation in morphological neural networks," *IEEE Transactions on Pattern Analysis and Machine Intelligence*, 2023. DOI: 10.1109/TPAMI.2023.3290615

[18]. Joshi K., Patil B., "Prediction of surface roughness by machine vision using principal components-based regression analysis," *Procedia Computer Science*, 167, 382-391, 2020.

[19]. Öztürk O. B., Başar E., "Multiple linear regression analysis and artificial neural networks -based decision support system for energy efficiency in shipping," *Ocean Engineering*, 243, 110209, 2022.

[20]. Chen H., Wang B., Li J., Xu J., Zeng J., Gao W., Chen K., "Comparative study on the extraction efficiency, characterization, and bioactivities of Bletilla striata polysaccharides using response surface methodology (RSM) and genetic algorithm-artificial neural network (GA-ANN)," *International Journal of Biological Macromolecules*, 226, 982-995, 2023.

[21]. Lau H. L., Wong F. W. F., Abd Rahman R. N. Z. R., Mohamed M. S., Ariff A. B., Hii S. L., "Optimization of fermentation medium components by response surface methodology (RSM) and artificial neural network hybrid with genetic algorithm (ANN-GA) for lipase production by Burkholderia cenocepacia ST8 using used automotive engine oil as substrate," *Biocatalysis and Agricultural Biotechnology*, 50, 102696, 2023.

[22]. Çelik Y. H., Fidan Ş., "Analysis of cutting parameters on tool wear in turning of Ti-6Al-4V alloy by multiple linear regression and genetic expression programming methods," *Measurement*, 200, 111638, 2022.